

# Electrochemical intercalation of sulphuric acid into CrO<sub>3</sub>-graphite intercalation compounds in aqueous solution

J. M. SKOWROŃSKI, K. JUREWICZ

*Institute of Chemistry and Applied Electrochemistry, Technical University of Poznań, ul. Piotrowo 3, 60–965 Poznań, Poland*

Received 6 June 1991; revised 14 October 1991

The electrochemical process of intercalation-deintercalation of sulphuric acid into chromium trioxide-graphite intercalation compounds (CrO<sub>3</sub>-GICs) has been studied using 12 M H<sub>2</sub>SO<sub>4</sub>. It is shown that the anodic oxidation reactions of CrO<sub>3</sub>-GICs and cathodic reduction of the product of anodization are different when compared to those occurring in the pure graphite. The differences in the slow cyclic potentiodynamic curves, depending on the method of preparation of CrO<sub>3</sub>-GICs, are considered. The practical implications of the electrochemical transformation of CrO<sub>3</sub>-GIC for battery applications are shown.

## 1. Introduction

Previously much attention has been paid to the electrochemical intercalation of graphite by sulphuric acid [1–17]. The formation of H<sub>2</sub>SO<sub>2</sub>-graphite intercalation compounds (H<sub>2</sub>SO<sub>4</sub>-GICs) is a reversible reaction if the process occurs in concentrated (18 M) sulphuric acid. On diluting the acid the formation of the saturated stage 1 compound becomes more and more difficult and the reversibility of the reaction decreases due to the anodic side reactions and corrosion effects [8, 11, 15, 16]. More recently it has been reported that the mechanism of the H<sub>2</sub>SO<sub>4</sub> intercalation changes in concentrated acid if CrO<sub>3</sub>-graphite intercalation compound (CrO<sub>3</sub>-GIC) is used instead of pure graphite [17]. Among others, H<sub>2</sub>SO<sub>4</sub>-GICs of the stage higher than 1 are produced galvanostatically with distinctly lower anodic charge (even over 30%) whereas the dramatic cathodic jump appears suddenly [17] on the anodic branch of the first potentiodynamic cycle within the potential range of the stage 2 to 1 transformation. This effect has been attributed to the opening of the graphite pockets enclosing the CrO<sub>3</sub> intercalate, by the cointercalating H<sub>2</sub>SO<sub>4</sub>, followed by flake exfoliation. This interpretation is consistent with an abrupt decrease of the in-plane electrical conductivity at the potential of the cathodic jump [18].

In the present work results for the intercalation-deintercalation of sulphuric acid into CrO<sub>3</sub>-GIC performed in 12 M H<sub>2</sub>SO<sub>4</sub> are reported. The results of slow cyclic potentiodynamic measurements are considered in terms of the changes occurring in CrO<sub>3</sub>-GICs of different structure due to cointercalation of H<sub>2</sub>SO<sub>4</sub>.

## 2. Experimental details

CrO<sub>3</sub>-GICs were prepared by the solvent and the impregnation-dry method. Intercalation by the for-

mer method was carried out according to the procedure of Platzer and de la Martinière [19], using a mixture of 1 g graphite and 5 g CrO<sub>3</sub>, in 50 cm<sup>3</sup> glacial acetic acid. The product was washed with acetone and dried to constant weight. The procedure of the impregnation-dry method has been described earlier in detail [20]. To remove unreacted CrO<sub>3</sub> and lower non-intercalated chromium oxides, the product of this method was washed with boiling water and 6 M HCl at 100°C for 1 h. Finally, washing with boiling water was continued until the Cr(VI) ion concentration in the filtrate was lower than  $5 \times 10^{-2} \mu\text{g cm}^{-3}$ ; then the sample was washed with acetone and dried to constant weight.

X-ray diffraction analysis was performed using CuK $\alpha$  radiation. The preparation, chemical analysis and X-ray data of the compounds are listed in Table 1.

Unless stated otherwise, the electrochemical studies were performed in 12 M H<sub>2</sub>SO<sub>4</sub> using an H-type cell in which the working and the counter electrode compartments were separated by a glass frit. The working electrode, in the form of a particle bed, was placed on a platinum screen. To ensure a good electrical contact between the graphite particles, a short glass cylinder, closed at its bottom by a polypropylene fibre, was placed at the top of the electrode. The counter electrode was a platinum spring whereas the reference was a Hg/Hg<sub>2</sub>SO<sub>4</sub> electrode filled with 1 M H<sub>2</sub>SO<sub>4</sub> and connected to the solution under investigation by a Luggin capillary. Potentials measured against this electrode are designated *E* in all figures of this paper. The potentiodynamic measurements were initiated at the rest potential of the electrode and a potential was changed in the positive direction until a potential of 0.95 or 1.15 V was reached. Then the direction of polarization was reversed and the potential was reduced down to –0.05 V. From this potential a new cycle in the positive direction was carried out. All

Table 1. Preparation, chemical analysis and X-ray data

Sample*	Intercalation method	C/Cr	Main graphite and intercalation lines	
			d/nm	I/I <sub>0</sub>
A2-AC	Solvent method [19]. Graphite flakes (99.7 wt % C) from Graphitwerke Kropfmühl AG, 170–283 $\mu\text{m}$ diameter (sample A2).	43.8	0.335 <sup>†</sup> 0.360	100 95
A1-W1	Impregnation-dry method [20]. Graphite flakes (99.7 wt % C) from Graphitwerke Kropfmühl AG with 95 wt % flakes in the range 170–544 $\mu\text{m}$ (sample A1).	28.1	0.335 0.352 <sup>‡</sup>	100 17

\* All symbols of samples are the same as in our previous papers.

<sup>†</sup> The complete XRD pattern is presented in ref. [28].

<sup>‡</sup> This broad peak appearing in the range 0.351–0.363 nm is probably composed of many components of mixed-stage structures. Evidence for intercalation by indirect methods is summarized in [28].

measurements were performed at a temperature of 20°C using the electrode weight of 50 mg.

### 3. Results and discussion

There are some differences in the process of intercalation of graphite with  $\text{H}_2\text{SO}_4$  depending on the molar concentration of acid. On decreasing the electrolyte concentration the intercalation potential (the potential at which the current begins to rise steeply [8]) increases linearly and side reactions, effected by the interaction of sample with water, become more and more competitive [8, 11, 15, 16]. It has been shown, however, by Beck *et al.* [4, 8, 10, 11] that in 12 M  $\text{H}_2\text{SO}_4$  the corrosion rate is almost as low as in 18 M  $\text{H}_2\text{SO}_4$  and unexpectedly low for bed electrodes [5, 11]. The potentiodynamic curves obtained for bed electrodes (Fig. 1) are similar to those reported earlier by other authors for the polypropylene bonded graphite electrodes (CPP) [8, 10] and the resolution of current peaks is satisfying. It is reasonable to note at this point that potentiodynamic curves of good quality can always be recorded for bed electrodes, even when the graphite particles are not pressed, if suitable experimental conditions are used (among others, possibly low scan rate, small thickness of the particle bed, a good electrical contact between a platinum collector and the graphite bed) [20–25].

It has been reported more recently [17] that if  $\text{CrO}_3$ -GICs are electrochemically intercalated in 18 M  $\text{H}_2\text{SO}_4$  instead of the pristine graphite then surprising effects are recorded on the potentiodynamic curves. During the first positive sweep one large sharp cathodic jump appeared at a potential nearly corresponding to the completion of the stage 1  $\text{H}_2\text{SO}_4$ -graphite compounds (about 0.9 V), and, in turn, after changing the direction of polarization a very large cathodic response was observed

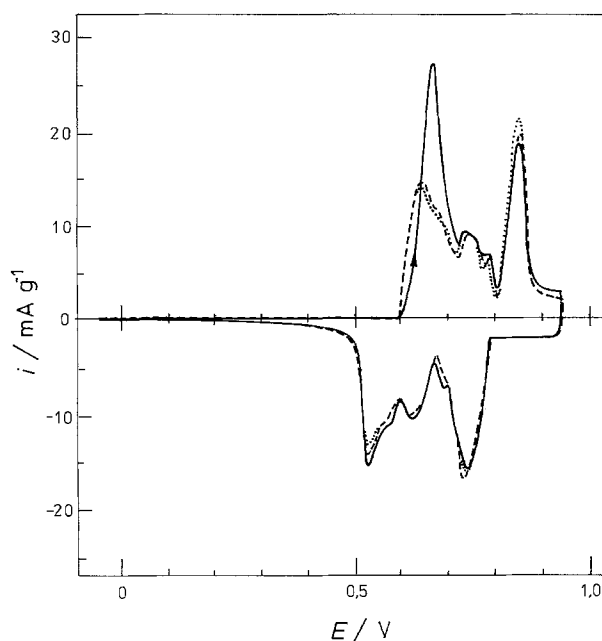


Fig. 1. Cyclic potentiodynamic curves obtained in 12  $\text{H}_2\text{SO}_4$  for pristine graphite (sample A1). Potential range  $-0.05$ – $0.95$  V; scan rate  $0.022$   $\text{mV s}^{-1}$ ; (—) cycle 1, (---) cycle 2, (····) cycle 3.

This unusual phenomenon is also recorded in the potentiodynamic curves obtained in 12 M  $\text{H}_2\text{SO}_4$  but the situation is more complicated as compared with that observed in 18 M  $\text{H}_2\text{SO}_4$ . During the first positive sweep of sample A1-W1 (Fig. 2), except for one cathodic jump appearing at 0.58 V, two cathodic peaks of distinctly smaller amplitude (at 0.66 and 0.80 V) are recorded. The comparison of Figs 1 and 2 shows that the first cathodic jump appears instantly when the intercalation process begins. In the case of sample

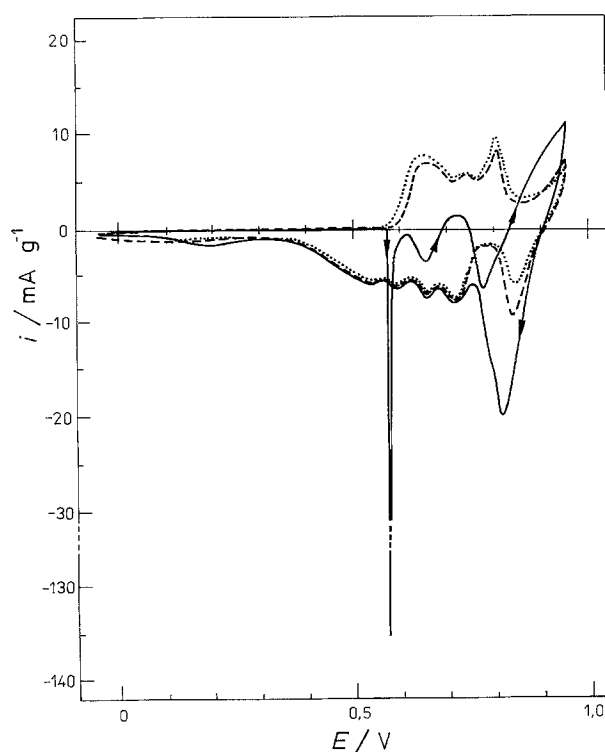


Fig. 2. Cyclic potentiodynamic curves obtained in 12 M  $\text{H}_2\text{SO}_4$  for  $\text{CrO}_3$ -GIC (sample A1-W1). Potential range  $-0.05$ – $0.95$  V; scan rate  $0.022$   $\text{mV s}^{-1}$ ; (—) cycle 1, (---) cycle 2, (····) cycle 3.

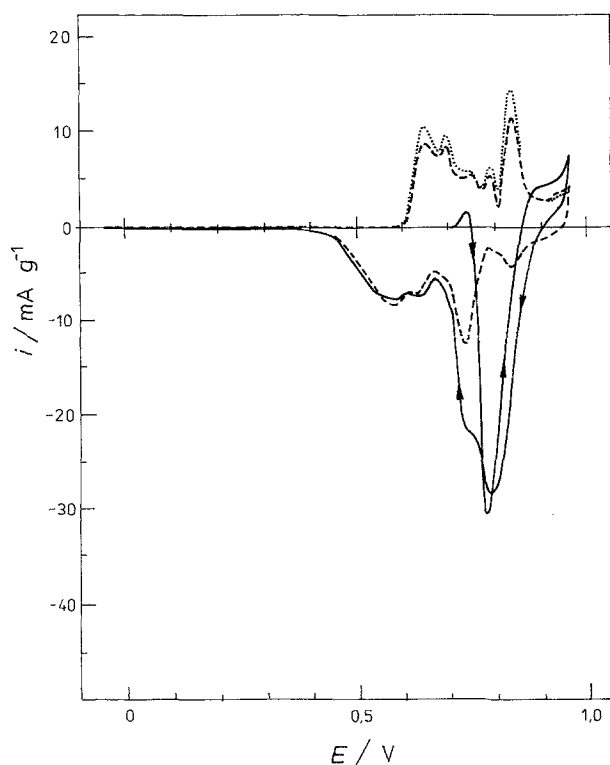


Fig. 3. Cyclic potentiodynamic curves obtained in 12 M H<sub>2</sub>SO<sub>4</sub> for CrO<sub>3</sub>-GIC (sample A2-AC). Potential range -0.05-0.95 V; scan rate 0.022 mV s<sup>-1</sup>; (—) cycle 1, (---) cycle 2, (····) cycle 3.

A2-AC (Fig. 3) only the last cathodic jump at 0.78 V is observed because the rest potential of this electrode is higher than the potentials corresponding to the first two peaks noted for sample A1-W1. However, after the polarization is reversed a large cathodic response is noted for both intercalation compounds. To investigate the mechanism of these surprising effects the measurements were performed using modified experimental conditions. First, if sample A1-W1 prior to the measurements was immersed in the electrolyte as long as 95 h, no changes in the potentiodynamic curves were observed. On this basis it may be assumed that the cathodic jumps are not caused by chemical dissolution of CrO<sub>3</sub>-GIC but exclusively depend on the potential imposed on the electrode. Secondly, if at the moment when the first cathodic shoot appeared on the potentiodynamic curve the potential sweep was stopped, and after 55 h started again in the positive direction, then in the potentiodynamic curve the second jump disappeared whereas the third one remained unchanged (Fig. 4).

As mentioned above, the cathodic effect appearing during the anodic oxidation of CrO<sub>3</sub>-GICs in 18 M H<sub>2</sub>SO<sub>4</sub> has been accounted for by the opening of the graphite pockets encapsulating the intercalate [23, 25-27] due to cointercalated of sulphuric acid [17, 18]. The question still remains whether the ternary CrO<sub>3</sub>-H<sub>2</sub>SO<sub>2</sub>-graphite compound (stable or intermediate) is formed or the intercalated CrO<sub>3</sub> (and/or lower chromium oxides [22-24] residing between the graphite interspaces) reacts with, or is replaced by, bisulphate ions solvated with neutral molecules of H<sub>2</sub>SO<sub>4</sub>. It is, however, without any doubt that in every

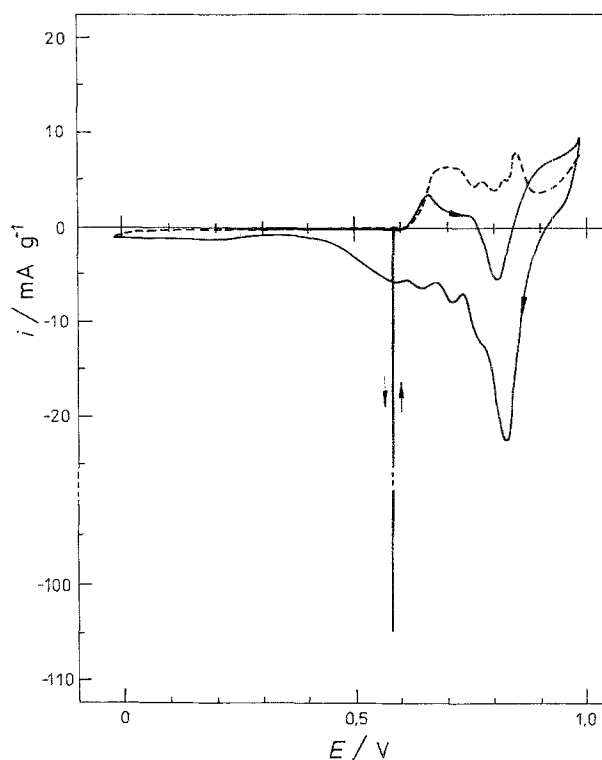


Fig. 4. Cyclic potentiodynamic curves obtained in 12 M H<sub>2</sub>SO<sub>4</sub> for CrO<sub>3</sub>-GIC (sample A1-W1). Potential range -0.05-0.95 V. Scan rate 0.022 mV s<sup>-1</sup>; (—) cycle 1 (potential was stopped at the point of the first cathodic jump for 55 h and then started again), (---) cycle 2.

case the electrode potential rises immediately when the cointercalating H<sub>2</sub>SO<sub>4</sub> reaches the chromium intercalate and the path between the electrolyte and the CrO<sub>3</sub> island is opened. In this way, the fixed potential can significantly exceed the potential imposed on the electrode by the generator. In consequence, the resulting cathodic current is recorded while the anodic intercalation of sulphuric acid proceeds in parallel. The cathodic jump phenomenon can be simulated for pristine graphite if, during the anodic run, the electrolyte containing the dissolved CrO<sub>3</sub> is injected into the bed electrode.

Although the process examined in this work in aqueous solution differs to some extent from that observed in 18 M sulphuric acid, nevertheless the reactions responsible for the cathodic jumps can be understood based on the above mechanism provided that several additional factors are taken into consideration. The first difference is that instead of one cathodic jump proceeding in concentrated acid for CrO<sub>3</sub>-GICs prepared by both methods of intercalation, in aqueous solution three cathodic peaks are observed for the compound prepared by the impregnation-dry method (sample A1-W1) (Fig. 2). As mentioned above, in the case of the compound prepared by the solvent method (A2-AC) only one cathodic peak was recorded (Fig. 3) due to the fact that the rest potential of the sample was higher than the potentials of the first two peaks. Because sample A2-AC is partially deintercalated with water, in contrast with sample A1-W1 [23], it is likely that, before the potential scan is started, CrO<sub>3</sub>

deintercalated from the outer regions of flakes increasing the electrode potential, results in the formation of the higher stage  $\text{H}_2\text{SO}_4$ -graphite compound.

Whether or not the number of peaks recorded actually corresponds to the three-step reaction mechanism may be considered in the light of the following results. The shape of the cathodic peaks suggests that the first jump at 0.58 V is a very fast reaction whereas the following cathodic peaks are related to the diffusion rate controlled reactions. According to the mechanism proposed earlier [17, 18] the major jump is associated with opening of the graphite pockets encapsulating the intercalate islands. The released and then hydrolysed  $\text{CrO}_3$  and/or lower chromium oxides, increasing the sample potential over that of the generator, are then rapidly reduced. The results obtained show that the cathodic jump takes place in 12 M  $\text{H}_2\text{SO}_4$  when the intercalation of  $\text{H}_2\text{SO}_4$  begins whereas in concentrated acid [17, 18] this effect is not observed before the stage 2  $\text{H}_2\text{SO}_4$ -graphite compound is formed. This fact makes it clear that the presence of water in the electrolyte facilitates this process. As mentioned above, if after a very long potential hold of the sample A1-W1 at the potential of the first jump (55 h) the forward potential sweep is again continued in the positive direction (Fig. 4) then the second jump disappears whereas the last cathodic peak remains unchanged (even after distinctly longer times of potentiostatic treatment, for example one week). On the other hand, the anodic peak appearing in Fig. 4, at the potential where the second cathodic jump was present in Fig. 2, is distinctly smaller in intensity as compared with that recorded in the same potential region during the first anodic sweep of the pristine graphite (Fig. 1) as well as during the second anodic sweep of sample A1-W1 (Fig. 2). This suggests that the cathodic reaction corresponding to the second cathodic peak begins in the region of the first cathodic jump and the peak current noted during the first anodic sweep results from the superposition of the anodic and cathodic processes proceeding simultaneously.

If it is assumed that the reactions responsible for the appearance of the second and the third cathodic peaks are governed by diffusion, then it may be expected that these cathodic effects will decrease on increasing the scan rate. The potentiodynamic curves obtained using a higher scan rate of  $0.1 \text{ mV s}^{-1}$  support the above assumption. It is well known that intercalation of  $\text{H}_2\text{SO}_4$  into the pure graphite is governed by diffusion and it is obvious that in the case of sample A1 (Fig. 5) the increase in the scan rate results, not only in the increase of the peak current and shifting of the anodic peaks towards more positive potentials and the cathodic ones towards more negative potentials, but also makes the peaks wider. Very interesting changes are observed in Figs. 6 and 7 obtained for  $\text{CrO}_3$ -GICs. For the first anodic scan of sample A1-W1 the third cathodic peak noted in Fig. 2 is transferred to the anodic current side in Fig. 6. For sample A2-AC (Fig. 7) no cathodic peaks are recorded and the first main and double anodic peak observed in the range

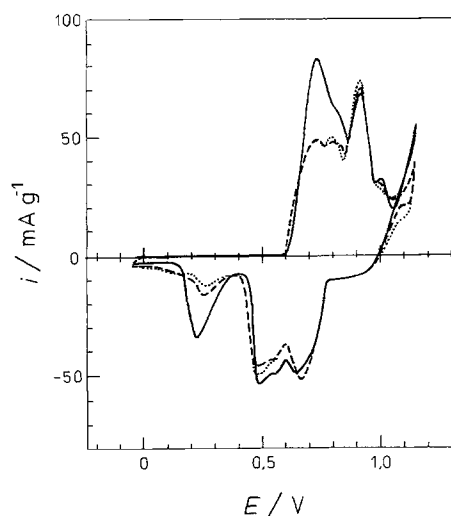


Fig. 5. Cyclic potentiodynamic curves obtained in 12 M  $\text{H}_2\text{SO}_4$  for pristine graphite (sample A1). Potential range  $-0.05$ – $1.15$  V; scan rate  $0.1 \text{ mV s}^{-1}$ ; (—) cycle 1, (---) cycle 2, (···) cycle 3.

$0.6$ – $0.9$  V for the pristine graphite (Fig. 5) is not present. In spite of the disappearance of the cathodic jumps on the anodic curves the occurrence of the reaction involving the intercalated  $\text{CrO}_3$  is demonstrated by a large cathodic peak formed instantly after the reversal of polarization in the negative direction. In agreement with the results obtained in concentrated  $\text{H}_2\text{SO}_4$  [17, 18] the cathodic current jumps also appearing in 12 M  $\text{H}_2\text{SO}_4$  during the first anodic oxidation of  $\text{CrO}_3$ -GICs can be attributed to the reactions of  $\text{CrO}_3$  intercalated in graphite by the impregnation-dry as well as the solvent method. The differences observed in the electrochemical behavior of the examined compounds can be attributed to their structural and chemical properties [23, 28]. In the case

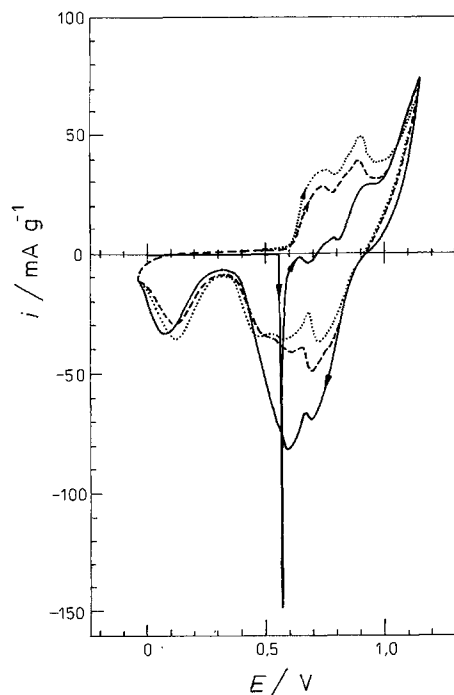


Fig. 6. Cyclic potentiodynamic curves obtained in 12 M  $\text{H}_2\text{SO}_4$  for  $\text{CrO}_3$ -GIC (sample A1-W1). Potential range  $-0.05$ – $1.15$  V; scan rate  $0.1 \text{ mV s}^{-1}$ ; (—) cycle 1, (---) cycle 2, (···) cycle 3.

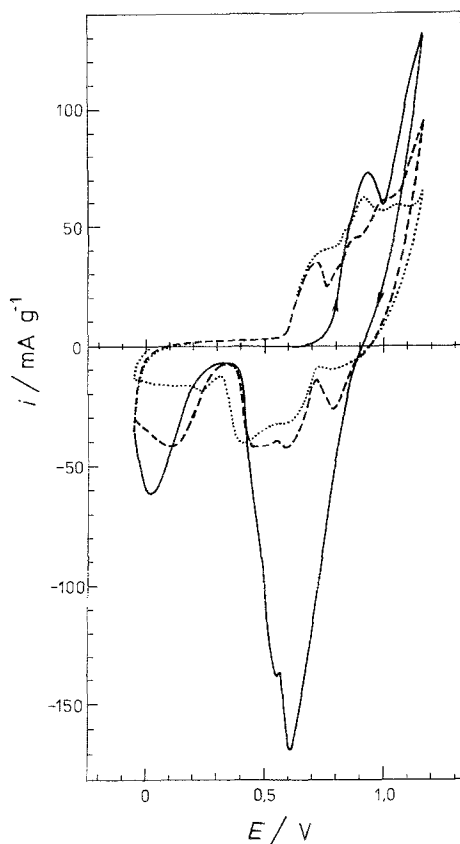


Fig. 7. Cyclic potentiodynamic curves obtained in 12 M H<sub>2</sub>SO<sub>4</sub> for CrO<sub>3</sub>-GIC (sample A2-AC). Potential range -0.05-1.15 V; scan rate 0.1 mV s<sup>-1</sup>; (—) cycle 1, (---) cycle 2, (···) cycle 3.

of sample A2-AC (Fig. 3) the curves of the second and third cycle do not differ and are similar to the curves obtained for the pristine graphite (Fig. 1 represents the pristine graphite A1; however the curves obtained for the pristine graphite A2 of smaller particles are substantially the same [17], which suggests that during the first cycle all intercalate is released from the graphite structure. For sample A1-W1 (Fig. 2) the anodic peaks remain relatively broad and the ratio of their amplitudes is different from those of the pristine graphite (Fig. 2). Although it is not possible to give more comprehensive explanation for several cathodic jumps recorded for sample A1-W1 nevertheless taking into account the fact that this sample is of very disordered structure [22-24, 28] it may be assumed that the following jumps may be related to the reaction of intercalate of a different energy bonding. This hypothesis is supported by the fact that the cathodic peak recorded at about 0.8 V during the cathodic sweep and attributed to the reduction of the intercalate released from the graphite structure is present on the potentiodynamic curves of sample A1-W1 for several cycles, whereas it disappears after the second cycle for sample A2-AC. A similar property has also been observed in 18 M H<sub>2</sub>SO<sub>4</sub> [17] and was attributed to the fact that the compound prepared by the impregnation-dry method is more resistant to deintercalation due to its more disordered structure with the island-type intercalate as compared with

a well ordered compound prepared by the solvent method [22, 23, 27].

The results of the present work show that the presence of water in the electrolyte accelerates the process of deintercalation of CrO<sub>3</sub>-GICs during intercalation of sulphuric acid. The interaction of water with H<sub>2</sub>SO<sub>4</sub>-graphite compounds has been studied earlier by several groups. In the literature there is an agreement that the stability of the compounds deteriorates on "hydrolysis" [4, 5, 8, 11, 15, 16]. The possibility of discharging the CrO<sub>3</sub> intercalate in aqueous electrolytes could, in future, be utilized in the field of chemical power sources, for example in reserve cells. On the other hand, GICs play a role as precursor for the graphite oxide in the presence of water [29, 30]. This work confirms the findings reported earlier [16, 31, 32] that in dilute sulphuric acid graphite oxide can be easily prepared by the electrochemical method. The potential range corresponding to the formation of graphite oxide begins at potentials following the completion of the stage 2 H<sub>2</sub>SO<sub>4</sub>-compound, about 0.95 V (Fig. 5). Although this potential is roughly the same for CrO<sub>3</sub>-GICs used instead of the pristine graphite (Figs. 6 and 7), several interesting differences are observed. The cathodic reduction of graphite oxides takes place with large overpotential and its value is smaller in the process using the pristine graphite (the cathodic peak at 0.25 V) (Fig. 5) as compared with that involving CrO<sub>3</sub>-GICs (for the first discharge the maximum of the peak is observed at a potential of 0.1 V both for sample A1-W1 and A2-AC (Figs 6 and 7)). However it is worth noting that the overpotential of the reduction of graphite oxide obtained from the CrO<sub>3</sub>-H<sub>2</sub>SO<sub>4</sub> precursor decreases distinctly on cycling. From the practical point of view a very useful property is that the charge gained from the discharge of graphite oxide is distinctly greater if the oxide is prepared by the overoxidation of the CrO<sub>3</sub>-H<sub>2</sub>SO<sub>4</sub>-graphite system. The problem related to the formation of graphite oxide mentioned here will be considered in more detail in a subsequent paper.

#### Acknowledgements

Financial support of this work by the Central Research Program CPBP No. 01.15 is gratefully acknowledged.

#### References

- [1] W. Rüdorff and U. Hofmann, *Z. Anorg. Allg. Chem.* **238** (1938) 1.
- [2] F. Beck, H. Junge and H. Krohn, *Electrochim. Acta* **26** (1981) 799.
- [3] A. Metrot and J. F. Fischer, *Synth. Met.* **3** (1981) 201.
- [4] F. Beck, H. Krohn and W. Kaiser, *J. Appl. Electrochem.* **12** (1982) 610.
- [5] H. Krohn, F. Beck and R. Herman, *Chem. Ing. Techn.* **54** (1982) 530.
- [6] L. E. A. Berlouis and D. J. Schiffrin, *J. Appl. Electrochem.* **13** (1983) 147.
- [7] J. O. Besenhard, E. Wudy, H. Möhwald, J. Nickl, W. Biberacher and W. Foag, *Synth. Met.* **7** (1983) 185.
- [8] F. Beck and H. Krohn, *ibid.* **7** (1983) 193.
- [9] A. Metrot and H. Fuzelier, *Carbon* **22** (1984) 131.
- [10] F. Beck and H. Krohn, *Synth. Met.* **14** (1986) 137.

- [11] F. Beck, H. Krohn and E. Zimmer, *Electrochim. Acta* **31** (1986) 371.
- [12] H. Shioyama and R. Fujii, *Carbon* **25** (1987) 771.
- [13] Y. Yosida and S. Tanuma, *Synth. Met.* **34** (1989) 341.
- [14] A. Harrach, C. Nicollin and A. Metrot, *ibid.* **34** (1989) 467.
- [15] J. O. Besenhard, J. Jacob, P. Möller, R. F. Sauter, A. D. Jannakondakis and A. Kurtze, *ibid.* **34** (1989) 719.
- [16] J. O. Besenhard, P. Minderer and H. Bindl, *ibid.* **34** (1989) 133.
- [17] J. M. Skowroński and K. Jurewicz, *ibid.* **40** (1991) 161.
- [18] J. M. Skowroński, J. Douglade and A. Metrot, Proceedings of the 6th International Symposium on Intercalation Compounds, Orleans, (1991).
- [19] N. Platzer and B. de la Martinière, *Bull. Soc. Chim. France* **197** (1961).
- [20] J. M. Skowroński, *Carbon* **24** (1986) 185.
- [21] *Idem*, *Electrochim. Acta* **30** (1985) 989.
- [22] *Idem*, *ibid.* **32** (1987) 1285.
- [23] *Idem*, *Synth. Met.* **22** (1987) 157.
- [24] *Idem*, *Electrochim. Acta* **33** (1988) 953.
- [25] *Idem*, *J. Power Sources* **32** (1990) 195.
- [26] *Idem*, *ibid.* **25** (1989) 133.
- [27] *Idem*, *Mat. Chem. Phys.* **24** (1990) 269.
- [28] *Idem*, *Carbon* **27** (1989) 537.
- [29] M. J. Bottomley, G. S. Parry, A. R. Ubbelohde and D. A. Young, *J. Chem. Soc.* **5674** (1963).
- [30] H. P. Boehm, M. Eckel and W. Scholz, *Z. Anorg. Allg. Chem.* **353** (1967) 236.
- [31] J. O. Besenhard, M. Bindl and H. Möhwald, Proceedings of the 4th Carbon Conference, Baden-Baden (1986) pp. 414-16.
- [32] F. Beck and H. Krohn, in 'The Electrochemistry of Carbon' (edited by S. Sarangapani, J. R. Akridge and B. Schumm), The Electrochemical Society, Pennington, NJ (1984).